The Astrophysical Journal Letters, 897:L26 (6pp), 2020 July 10 https://doi.org/10.3847/2041-8213/ab9f99
© 2020. The American Astronomical Society. All rights reserved.

Detection of Periodicity in SiO Maser Intensity and Velocity Shift of the Symbiotic Star CH Cyg

Se-Hyung Cho[1,2], Haneul Yang[2], Youngjoo Yun[2], Dong-Hwan Yoon[2], Jaeheon Kim[3], and Dong-Jin Kim[4]
[1] Astronomy program, Department of Physics and Astronomy, Seoul National University, Seoul 08826, Republic of Korea; cho@kasi.re.kr
[2] Korea Astronomy and Space Science Institute, Yuseong–gu, Daejeon 34055, Republic of Korea
[3] Department of Astronomy and Space Science, Chungbuk National University, Cheongju 28644, Republic of Korea
[4] Max-Planck-Institut fu¨r Radioastronomie, Auf dem Hügel 69, D-53121 Bonn, Germany
Received 2020 May 21; revised 2020 June 11; accepted 2020 June 22; published 2020 July 9

Abstract

We performed simultaneous monitoring observations of H_2O 6_{16}–5_{23} and SiO $v = 1, 2$, $J = 1 \rightarrow 0$, SiO $v = 1$, $J = 2 \rightarrow 1, 3 \rightarrow 2$ maser lines toward the symbiotic star CH Cyg from 2012 December to 2019 November using the Korean very long baseline interferometry Network single-dish telescope. SiO $v = 1, 2$, $J = 1 \rightarrow 0$ and $v = 1$, $J = 2 \rightarrow 1$ maser lines were detected for the first time. A periodicity of about 2.5 yr in the SiO maser intensity was found, showing its association with the pulsation of the M giant in CH Cyg. Only the SiO $v = 2$, $J = 1 \rightarrow 0$ maser, without detections of the $v = 1$, $J = 1 \rightarrow 0$ maser, was detected in 6 epochs out of 15 $v = 2$, $J = 1$–0 maser detected epochs. In addition, the SiO $v = 1$, $J = 2 \rightarrow 1$ maser intensity was always stronger than that of the $v = 1$, $J = 1 \rightarrow 0$ maser except for one epoch, providing a critical constraint on the different masing conditions by different transitions, according to changes of the CH Cyg symbiotic system. We also found the gradual redshifted peak velocities of the SiO masers had about a 2.5 yr periodicity corresponding to the period of peak intensities (redshifted up to about +40 km s^{-1} with respect to the stellar velocity of the M giant). Two possible explanations can be suggested for the 2.5 yr period of the SiO maser intensity and velocity behaviors, although their actual causes remain uncertain.

Unified Astronomy Thesaurus concepts: Symbiotic binary stars (1674); Silicon monoxide masers (1458); Circumstellar masers (240); Roche lobe overflow (2155)

1. Introduction

Symbiotic systems are composed of a mass-losing cool red giant and generally a hot white dwarf companion. They are considered to be one of the agents responsible for breaking the spherically symmetric mass-loss envelope in the transient evolution phase from asymptotic giant branch stars to planetary nebulae (De Marco Orsola 2009). Additionally, symbiotic recurrent novae have been considered Type Ia supernova (SN Ia) progenitors (Hachisu & Kato 2001; Dilay et al. 2012). In symbiotic systems, the strong interactions between red giants and white dwarfs yield a number of interesting and complex phenomena, like accretions of the stellar material around the hot companion, the formation of bipolar outflows and jets, and so on. However, the details of their processes and structure are not well known.

Red giants in symbiotic systems usually exhibit weak molecular thermal and maser emission due to photodissociation by the UV radiation from the hot companion (Ivison et al. 1994; Seaquist et al. 1995). The CO thermal emissions coming from outer shells are extremely weak in symbiotic systems (for example, R Aqr and CH Cyg; Bujarrabal et al. 2010). However, some symbiotic systems show relatively strong SiO and/or H_2O masers compared to thermal lines, both SiO and H_2O masers from the D-type (dust-type) symbiotic systems of o Ceti (Wong et al. 2016), V627 Cas (Cho et al. 2018; Yang et al. 2020), R Aqr (Ivison et al. 1994; Kamohara et al. 2010), and SiO-only masers without a H_2O maser from the D-type symbiotic system V407 Cyg (Deguchi et al. 2011). The H_2O and SiO masers including SiO thermal emission can be a useful probe for investigating the position of red giants and interactions between hot and cool winds.

The S-type (stellar-type) symbiotic system CH Cyg (Belczyński et al. 2000) consists of a hot accreting white dwarf and mass-losing cool M6-7 III giant. The separation between the two components has been measured to be 42 mas by speckle interferometry (Mikoajewska et al. 2010). The distance of 244^{+49}_{-35} pc was obtained from Hipparcos data (van Leeuwen 2007). The distance based on Gaia data (Gaia Collaboration et al. 2018) is 183 ± 7 pc, which shows a difference compared to that from Hipparcos data. A powerful radio jet with a strong radio outburst was detected for the first time in 1984 (Taylor et al. 1986). The jet was also detected at X-ray and optical wavelengths (Karovska et al. 2007) in the northeast–southwest direction. In addition, CH Cyg shows a peculiar period of about 750 days in both photometric (Skopal et al. 2007) and radial velocity variations, together with an orbital period of 15.6 yr (Hinkle et al. 2009). Hinkle et al. (1993, 2009) suggested that the period of about 750 days is the orbital motion of a low-mass companion in close orbit to the M giant, as a triple system of CH Cyg or the period of nonradial pulsation of the red giant. The period of 750 days is still under debate (Pedretti et al. 2009). Using the Korean very long baseline interferometry (VLBI) Network (KVN), we performed simultaneous monitoring observations of H_2O and SiO masers in order to investigate the characteristics of maser properties and behaviors including the interaction between the M giant and hot companion in the complex symbiotic system CH Cyg.

The observations are presented in Section 2. The results and discussion are described in Sections 3 and 4, respectively. We summarize our findings in Section 5.

2. Observations

Simultaneous time-monitoring observations of H_2O 6_{16}–5_{23} (22.235080 GHz) and SiO $v = 1, 2$, $J = 1 \rightarrow 0$, SiO $v = 1$, $J = 2 \rightarrow 1$, $3 \rightarrow 2$ (43.122080, 42.820587, 86.243442, and

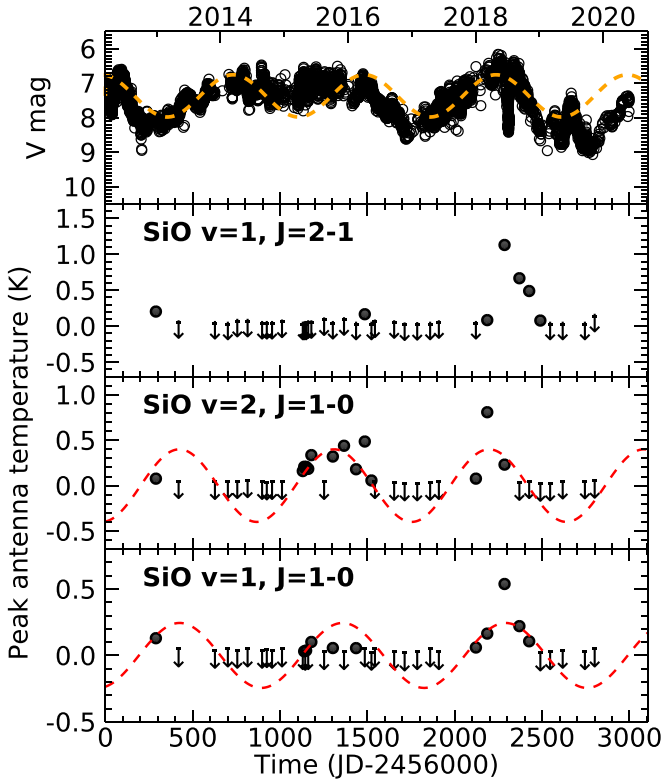

Figure 1. The peak antenna temperature variations of the SiO $v = 1$, 2, $J = 1 \rightarrow 0$ and $v = 1$, $J = 2 \rightarrow 1$ masers according to observational epochs from 2012 December 27 to 2019 January 6. The top panel shows corresponding optical V magnitude variations by AAVSO and the orange colored dashed line indicates the 750 day period fit of the M giant based on Skopal et al. (2007). The red colored dashed line shows a fitting result for the 2.5 yr period. The arrows indicate the 3σ upper limit of the KVN.

129.363359 GHz) maser lines toward CH Cyg were performed about every two months between 2012 December and 2019 November, as shown in Figure 1. We used the 21 m single-dish radio telescopes of the KVN equipped with a unique quasi-optics system for simultaneous observations of the $K/Q/W/D$ bands (Han et al. 2008). The average half power beam widths and aperture efficiencies were 123″, 0.58 (at 22 GHz) and 62″, 0.61 (at 43 GHz), 32″, 0.50 (at 86 GHz) and 23″, 0.35 (at 129 GHz), respectively.[5] The pointing accuracy was checked every 2 hr using χ Cyg. We used the cryogenic 22, 43, 86 GHz High Electron Mobility Transistor receivers and the Superconductor-Insulator-Superconductor 129 GHz receiver with both right and left circular polarized feeds (Han et al. 2013). Only the left circular polarized feed was used during our observations. The system noise temperatures of a single sideband ranged from 72 to 156 K (at 22 GHz), from 96 to 235 K (at 43 GHz), from 175 to 385 K (at 86 GHz), and from 189 to 566 K (at 129 GHz) depending on weather conditions and elevations. We used the digital spectrometer, which has a set of total bandwidths of three 32 MHz for the H_2O 6_{16}–5_{23}, SiO $v = 1$, 2, $J = 1 \rightarrow 0$, and two 64 MHz for SiO $v = 1$, $J = 2 \rightarrow 1$, $3 \rightarrow 2$, respectively. The total velocity ranges for four bands are about 411 km s^{-1} (at 22 GHz), 222 km s^{-1} (at 43 GHz), 222 km s^{-1} (at 86 GHz), and 148 km s^{-1} (at 129 GHz), respectively. The velocity resolutions were 0.11 km s^{-1} (at 22 GHz), 0.05 km s^{-1} (at 43 GHz), 0.05 km s^{-1} (at 86 GHz), and 0.04 km s^{-1} (at 129 GHz), respectively. All detected spectra at 22, 43, 42, and 86 GHz, except the spectrum of 43 GHz maser on 2015 June 5 (150605), were Hanning-smoothed for constant velocity resolutions of about 0.43 km s^{-1} ($\sim$1.72 km s^{-1} for the spectrum of 43 GHz maser on 150605).

The data calibration was achieved by the chopper wheel method, which corrects antenna gain variations and atmospheric attenuation, depending on elevation, in order to yield an antenna temperature T_A^*. The integration time to achieve a sensitivity of about 0.06 K was about 120 minutes at the 3σ level in position-switching mode. The average conversion factors from the antenna temperature to the flux density were about 13.8 Jy K^{-1} at 22 GHz, 13.1 Jy K^{-1} at 43 GHz, 15.9 Jy K^{-1} at 86 GHz, and 22.8 Jy K^{-1} at 129 GHz, respectively.

3. Results

Figure 1 shows the results of the detected peak antenna temperature and the upper limits of SiO $v = 1$, 2, $J = 1 \rightarrow 0$, and SiO $v = 1$, $J = 2 \rightarrow 1$ according to the optical light curve of CH Cyg from 2012 December to 2019 November. The H_2O and SiO $v = 1$, $J = 3 \rightarrow 2$ masers were not detected within their upper limits of 0.04 and 0.04 K during our monitoring observations. Table 1 displays the detected values of the peak antenna temperatures, including upper limits in the undetected lines and peak velocities of the SiO masers. From 2019 March to November, it entered the undetected phase again. The intensity maximum of the SiO masers between 2018 and 2019 appears around the optical maximum. The SiO $v = 2$, $J = 1 \rightarrow 0$ maser without the detection of the $v = 1$, $J = 1 \rightarrow 0$ maser was detected in epochs 150417, 150501, 150518, 151209, 160406, and 160514. On the other hand, the SiO $v = 1$, $J = 1 \rightarrow 0$ maser without the detection of the $v = 2$, $J = 1 \rightarrow 0$ maser was detected in epochs 180908 and 181103. In addition, the detected SiO $v = 1$, $J = 2 \rightarrow 1$ masers were always stronger than the $v = 1$, $J = 1 \rightarrow 0$ masers except for one epoch, 180309. These facts provide a critical constraint on the different masing conditions by different transitions of SiO masers depending on changes of the complex CH Cyg symbiotic system according to observational epochs. In Figure 1, we found a period of about 2.5 yr in the peak intensity variations of the SiO masers using MPFITFUN function with IDL (Markwardt 2009) (as a result of fitting by sinusoidal function, 2.56 ± 0.02 yr in the $v = 1$, $J = 1 \rightarrow 0$ maser and 2.43 ± 0.01 yr in the $v = 2$, $J = 1 \rightarrow 0$ maser). It was difficult to fit the peak intensity variations of the SiO masers with the 750 day period. The 2.5 yr period shows some differences from the peculiar period of about 750 days (2.1 yr) in both the photometric and radial variations of CH Cyg (Hinkle et al. 1993, 2009). The period of about 2.5 yr in the peak intensity variations of the SiO masers implies that they are associated with the pulsation motion of the M giant rather than the period of the orbital motion of the low-mass companion in close orbit to the M giant as a triple system. This is because SiO masers occur in the atmosphere of M giants and are directly influenced by stellar pulsation.

Figures 2 and 3 show the spectra of the SiO $v = 1$, 2, $J = 1 \rightarrow 0$ and $v = 1$, $J = 2 \rightarrow 1$ masers according to observational dates, respectively. They become increasingly redshifted from about stellar velocity $V_{LSR} = -60$ km s^{-1} (on 2012 December 27) to about $V_{LSR} = -21$ km s^{-1} ($v = 2$, $J = 1 \rightarrow 0$ maser on 2018 March 8) according to observational dates. These redshifted velocity features are well confirmed in

[5] https://radio.kasi.re.kr/kvn/main_kvn.php

Table 1
Peak Antenna Temperatures and Peak Velocities of SiO masers

Date	T_A^*(peak) (K)			V_{LSR}(peak) (km s^{-1})			Telescope
(yymmdd)	SiO ($J=1$–0)		SiO ($J=2$–1)	SiO ($J=1$–0)		SiO ($J=2$–1)	(Site)
	$v=1$	$v=2$	$v=1$	$v=1$	$v=2$	$v=1$	
(1)	(2)	(3)	(4)	(5)	(6)	(7)	(8)
2012 Dec 27	0.13	0.08	0.20	−60.3	−61.0	−59.2	KYS
2015 Apr 17	<0.04	0.16	<0.04	⋯	−49.7	⋯	KYS
2015 Apr 25	0.03	0.21	<0.04	−51.6	−49.3	⋯	KUS
2015 May 1	<0.03	0.19	<0.05	⋯	−48.8	⋯	KYS
2015 May 6	0.04	0.21	<0.03	−49.8	−48.3	⋯	KYS
2015 May 18	<0.05	0.18	<0.08	⋯	−47.7	⋯	KYS
2015 Jun 5	0.05	0.34	<0.08	−50.4	−46.2	⋯	KTN
2015 Oct 6	0.06	0.32	<0.06	−29.0	−27.9	⋯	KTN
2015 Dec 9	<0.04	0.44	<0.06	⋯	−22.9	⋯	KUS
2016 Feb 16	0.06	0.18	<0.04	−27.4	−22.0	⋯	KTN
2016 Apr 6	<0.08	0.49	0.17	⋯	−22.0	−25.1	KTN
2016 May 14	<0.03	0.06	<0.04	⋯	−22.0	⋯	KYS
2018 Jan 2	0.06	0.08	<0.05	−27.6	−23.0	⋯	KUS
2018 Mar 8	0.16	0.81	0.09	−26.5	−21.0	−25.8	KTN
2018 Jun 15	0.54	0.23	1.13	−25.8	−21.3	−25.8	KYS
2018 Sep 8	0.22	<0.04	0.67	−24.3	⋯	−22.2	KTN
2018 Nov 3	0.11	<0.05	0.49	−24.8	⋯	−24.4	KUS
2019 Jan 6	<0.02	<0.02	0.08	⋯	⋯	−26.5	KUS

Figure 4. The red colored arrow indicates the detected epochs in Figure 4. The values of the peak velocities of the SiO masers are given in Table 1. However, we could not detect blueshifted SiO maser emissions with respect to the stellar velocity during our observations. Interestingly, we also found the periodicity of the redshifted peak velocities of the SiO masers corresponded to the period of peak intensities (redshifted up to about +40 km s^{-1} with respect to the stellar velocity of the red giant −59.9 km s^{-1}) as shown in Figures 1 and 4. The SiO maser emission from single stars usually occurs around the stellar velocity, without showing such a large velocity shift. In the second cycle during 2015–2016, these gradual redshifted variations were clearly observed (Figure 4). In the first cycle of 2012 December, we detected the SiO maser emission near the stellar velocity in only one epoch because of limited observations. In the third cycle of 2018, only highly redshifted emission from −28 to −21 km s^{-1} was detected. In addition, we could not obtain the VLBI images of the SiO masers due to the limited sensitivity of KVN.

4. Discussions

We detected a periodicity of about 2.5 yr in the intensity variations of the SiO $v=1$, 2, $J=1\rightarrow0$ and $v=1$, $J=2\rightarrow1$ maser lines, and corresponding redshifted velocity features of the SiO masers during our monitoring observations (Figures 1 and 4). The 2.5 yr period of SiO masers showed a difference with previously known 750 day (Skopal et al. 2007) and 770 day (Mikolajewski et al. 1992) photometric periods and also with the 750 day (2.1 yr) radial velocity period found using 2 μm infrared observations (Hinkle et al. 1993). We do not yet know why there is a difference in the period although the SiO masers usually arise from 2 to 4 stellar radii of red giants (Diamond et al. 1994) above near-infrared regions. Hinkle et al. (1993) proposed that as a triple system of CH Cyg, the 750 day short-period is the orbital period of an inner binary system composed of the M giant and the unseen low-mass star. In contrast, Schmidt et al. (2006) suggested that the 750 day period is caused by a pulsation of the M giant, not by a close binary. Because the triple-system model has been controversial, Hinkle et al. (2009) suggested that the spectroscopic behavior of the 750 days velocity variation is consistent with long secondary-period variation of some semiregular variables and can be caused by two viable options, i.e., a low-order nonradial pulsation in the M giant, or a low-mass companion forming a common envelope with the M giant. He also suggested, as a naive expectation, that nonradial modes as a dominant mode might control stellar properties; for example, the mass-loss rate or the directionality of the mass loss, and a change in the mass transfer in a symbiotic system. Pedretti et al. (2009) detected asymmetry in CH Cyg with infrared interferometry, which was correlated with the phase of the 750 day period. They proposed that the combined effect of nonradial pulsation and a low-mass companion could explain the radial velocity curve of the 750 day period and the asymmetries.

Here, we compare the velocity behaviors of the 750 day orbital period in the inner binary system with those of our SiO masers. First, the semiamplitude of the velocity variation of the 750 day orbital period, compared to our large redshifted velocities of SiO masers (about +40 km s^{-1}), is very small (about ±2.6 km s^{-1}, Hinkle et al. 1993) with respect to the stellar velocity of the M star. It is strange if this is due to the same orbital motion of the 750 day orbital period. Therefore, the large difference between the semiamplitude of the orbital motion of the 750 day period and the redshifted velocities of SiO masers may be due to different causes.

Second, from 2013 to 2019 only the redshifted SiO maser emission was detected with respect to the stellar velocity of the M giant, as shown in Figures 2–4. These kinds of redshifted velocity behaviors with respect to the stellar velocity were also reported by Iijima et al. (2019). They reported that the narrow absorption lines of neutral metals, Fe I, Cr I, Ti I, etc., which

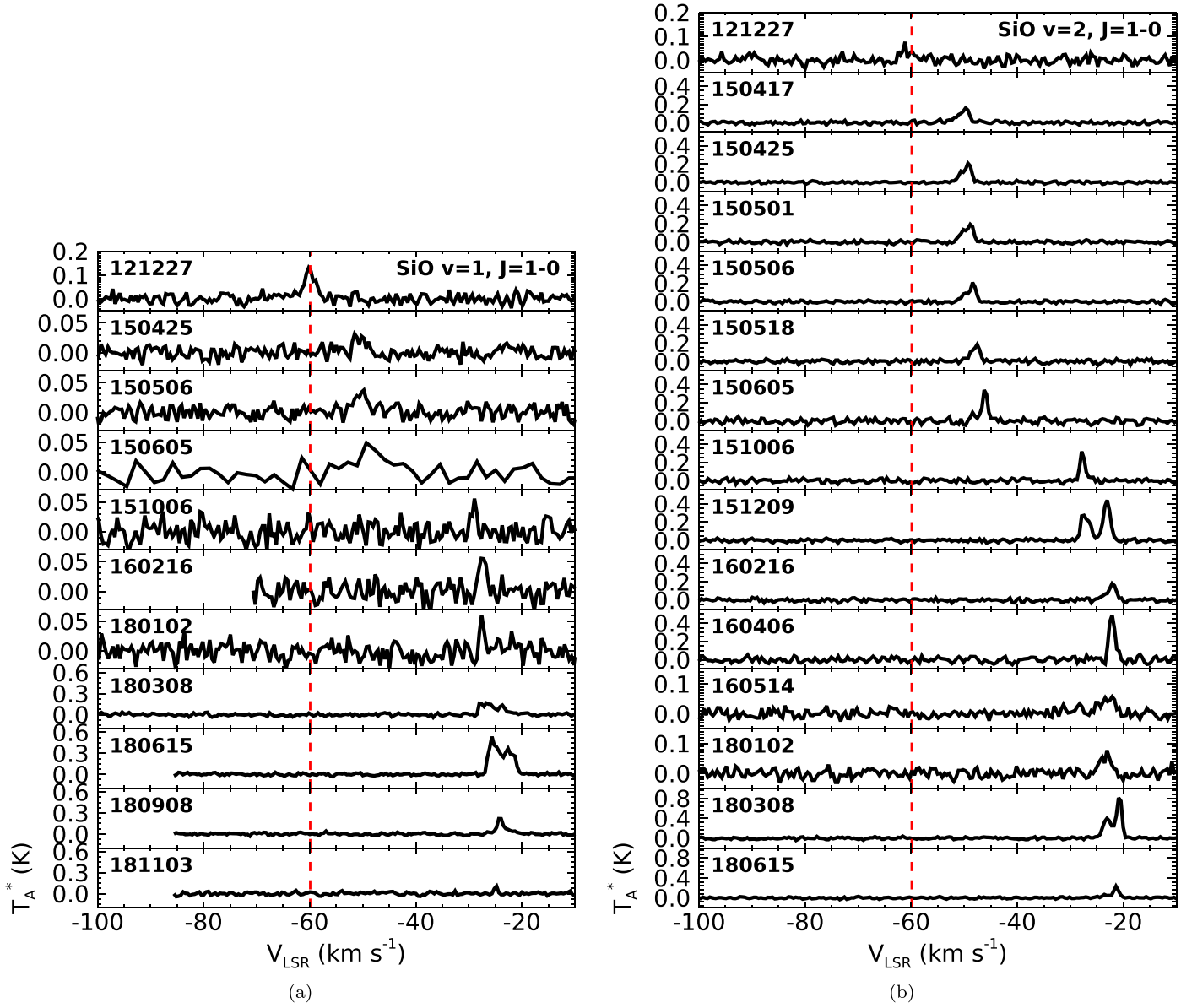

Figure 2. Variations in the SiO $v = 1, 2$, $J = 1 \rightarrow 0$ maser line profiles according to observational epochs from 2012 December 27 to 2018 November 3 (SiO $v = 1$, $J = 1 \rightarrow 0$) and 2018 June 15 (SiO, $v = 2$, $J = 1 \rightarrow 0$). The vertical dashed lines indicate the stellar velocity of CH Cyg ($V_{\rm LSR} = -59.9$ km s^{-1}, Hinkle et al. 2009).

appeared in 1998, can be clearly distinguished from those of the M giant, and were redshifted by about 30 km s^{-1} with respect to the absorption lines of the M giant. They regarded the narrow absorption lines as having been formed on the surface of the A-type dwarf, the hot companion of the inner binary, and their redshifts were due to the orbital motion of the hot companion with the 750 day period. Therefore, they suggested that their results seemed to support the Hinkle et al. (2009) triple system.

Iijima et al. (2019) also reported that the secondary absorption components of the Na I D1 and D2 lines began to appear at large redshifted velocities (from -13.2 to -20.6 km s^{-1}) with respect to the stellar velocity of the M giant ($V_{\rm LSR} = -59.9$ km s^{-1}) in 1998 July and August and gradually showed a blueshift of up to -75.2 km s^{-1} from 1998 December to 1999 March. Their radial velocities showed fairly large redshifted features with respect to the narrow absorption lines of the neutral metals (in the case of -17 km s^{-1}, redshifted by 15 km s^{-1}). They suggested the radial velocities of the secondary absorption lines varied with the orbital motion of the hot companion and were formed near the hot companion. In addition, the redshifted absorption components of the Na I lines coexisted with the high-velocity outflow during the active stage. They indicated that this fact might be related to high-velocity mass ejections along the orbital plane (namely, equatorial ejections), which are similar to those from rapidly rotating stars based on wind-compressed accretion disks (Owocki et al. 1994). However, their data on the narrow absorption lines of the neutral metals and the secondary absorption components of Na I D1 and D2 lines are limited, and mainly cover partial epochs showing relatively large redshifted velocities and $-58 \sim -75$ km s^{-1}.

The peak velocity variations of the SiO masers, including the amount of redshifted velocity in Figure 4, tend to be similar to those of the secondary absorption components of the Na I D1 and D2 lines in CH Cyg (Iijima et al. 2019). We can also adopt the existence of the low-mass companion in the inner binary system of a triple system (Hinkle et al. 1993; Iijima et al. 2019)

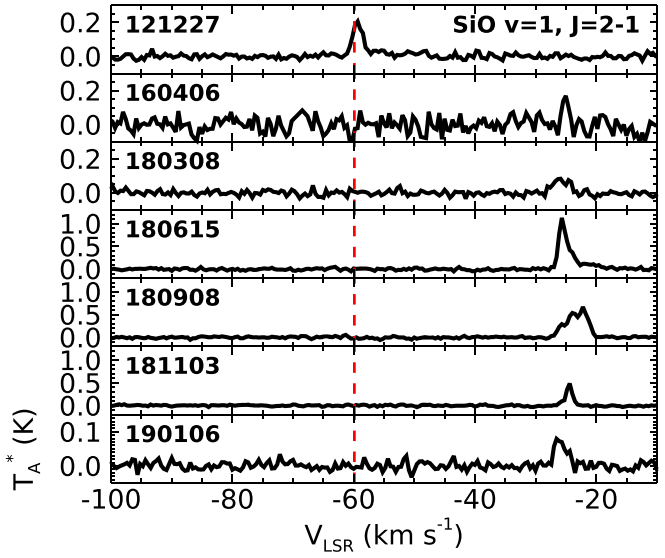

Figure 3. Variations in the SiO $v = 1$, $J = 2 \rightarrow 1$ maser line profiles according to observational epochs from 2012 December 27 to 2019 January 6. The vertical dashed line indicates the stellar velocity of CH Cyg ($V_{LSR} = -59.9$ km s^{-1}).

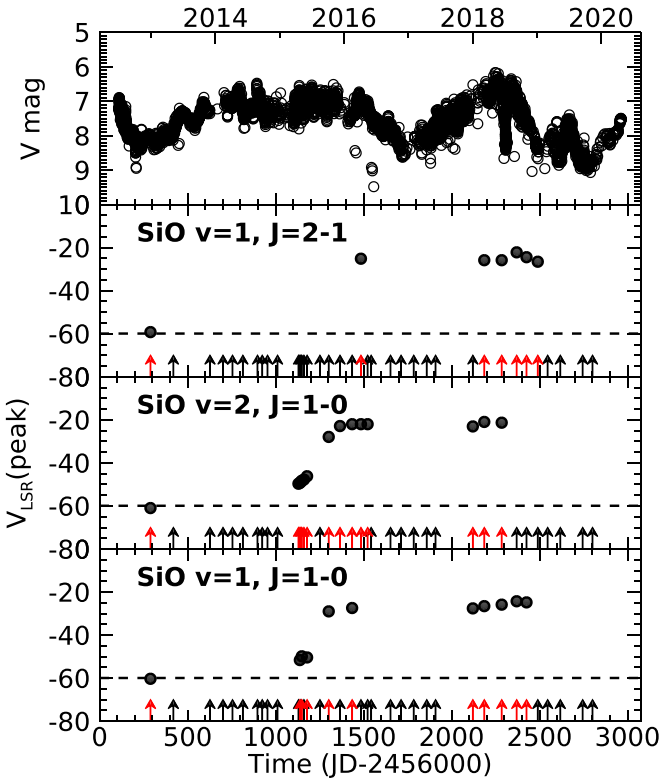

Figure 4. The peak velocity variations of the SiO $v = 1, 2$, $J = 1 \rightarrow 0$ and $v = 1$, $J = 2 \rightarrow 1$ masers according to observational epochs from 2012 December 27 to 2019 January 6. The top panel shows the corresponding optical V magnitude variations by AAVSO. The arrows indicate the observational epochs of KVN, and the red colored arrows indicate the detected epochs in the SiO maser lines. The horizontal dashed line indicates the stellar velocity of CH Cyg ($V_{LSR} = -59.9$ km s^{-1}).

as a possible explanation for the redshifted velocity behavior of the SiO masers. However, we did not detect the blueshifted velocity behavior of SiO masers as shown in Figures 2 and 3. Therefore, the 2.5 yr period of SiO maser intensities and velocity behaviors may be related to the periodic clumpy mass transfer in the binary system from the M giant to a low-mass companion due to a Roche lobe overflow at periastron. This kind of a periodic clumpy mass transfer will be stimulated by nonradial pulsation with a period of 750 days (Hinkle et al. 2009). In addition, because the ejected matter is clumpy, the physical conditions of high density and temperature may be satisfied for SiO masing inside the clump, according to pulsation phases. As another possibility, in the case this is a binary system not a triple system, the periodic redshifted velocity behaviors of the SiO masers may be a clumpy mass ejection from the M giant similar to the previously mentioned equatorial mass ejection, which is stimulated by nonradial pulsation with a period of 750 days. In any case, the causes of the 2.5 yr period of SiO maser intensity and velocity behaviors remain uncertain. In parallel with the single-dish long-term monitoring observations, a future interferometric observation to obtain detailed SiO maser spot maps near the binary stars at higher angular resolution and sensitivity is required to clarify the nature of the 2.5 yr period of SiO maser intensity and redshifted velocity behaviors in the symbiotic system CH Cyg.

The SiO $v = 2$, $J = 1 \rightarrow 0$ maser without the detection of the $v = 1$, $J = 1 \rightarrow 0$ maser was detected in 6 epochs in spite of higher vibrational state. After the epochs 180908 and 181103 reached the highest redshifted velocities, the $v = 1$, $J = 1 \rightarrow 0$ maser was detected, but the $v = 2$, $J = 1 \rightarrow 0$ was not. In addition, the detected SiO $v = 1$, $J = 2 \rightarrow 1$ maser was always stronger than the $v = 1$, $J = 1 \rightarrow 0$ maser except for one epoch 180308. The physical conditions for the different SiO maser lines were suggested based on the large velocity gradient model by Doel et al. (1995) and Goddi et al. (2009). They included both collisional and radiative pumping. Their results were that the SiO $v = 1, 2$, $J = 1 \rightarrow 0$ masers favor densities of 10^8–10^{10} cm^{-3}, kinetic temperatures higher than 1500 K ($v = 1$), and 10^9–10^{11} cm^{-3}, and kinetic temperatures higher than 2000 K ($v = 2$), respectively. Namely, the $v = 2$, $J = 1 \rightarrow 0$ maser was optimized at higher temperatures and more strongly inverted in a strong, hot radiation field than the $v = 1$ maser. In this regard, the $v = 2$, $J = 1 \rightarrow 0$ maser will be able to increase the gain by the cycling population via $v = 2$–0 absorption at 4 μm radiated by hot dust in CH Cyg and become stronger than $v = 1$. This is similar to the case with an increase of $v = 2$ only for masers and large values of the $v = 2/v = 1$ ratios in post-asymptotic giant branch stars related with the hot dust shell, as suggested by Yoon et al. (2014). The SiO $v = 1, 2$, $J = 1 \rightarrow 0$ masers were never inverted for $N_{H2} < 10^7$ cm^{-3} (Doel et al. 1995). The intensity of the $v = 1$, $J = 2 \rightarrow 1$ maser was always stronger than that of the $v = 1$, $J = 1 \rightarrow 0$ (Humphreys et al. 2002). The $v = 1$, $J = 2 \rightarrow 1$ maser occurred at slightly lower densities than those of the $v = 1$, $J = 1 \rightarrow 0$ (Richter et al. 2013; Issaoun et al. 2017). These masing conditions may be changed significantly in the clumpy mass transfer process associated with nonradial pulsation and the hot companion effect.

5. Summary

Using simultaneous monitoring observations of H_2O 6_{16}–5_{23} and SiO $v = 1, 2$, $J = 1 \rightarrow 0$, SiO $v = 1$, $J = 2 \rightarrow 1, 3 \rightarrow 2$ maser lines with the KVN single-dish telescope, we have detected the SiO $v = 1, 2$, $J = 1 \rightarrow 0$ and $v = 1$, $J = 2 \rightarrow 1$ maser lines and also a periodicity of about 2.5 yr in the SiO maser intensity and velocity shift toward the S-type symbiotic star CH Cyg for the first time. Only the SiO $v = 2$, $J = 1 \rightarrow 0$

maser, without detections of the $v = 1$, $J = 1 \rightarrow 0$ and $J = 2 \rightarrow 1$ masers, was detected in epochs 150417 (2015 April 17), 150501, 150518, 151209, 160406, and 160514. In addition, the SiO $v = 1$, $J = 2 \rightarrow 1$ maser intensity was always stronger than that of the $v = 1$, $J = 1 \rightarrow 0$ maser except for one epoch, 180308. These results place a critical constraint on the different masing conditions, suggesting different transitions of the SiO masers depending on changes of the complex CH Cyg symbiotic system. The period of $\sim$2.5 yr found in the peak intensity variations of SiO masers shows a difference with the reported 750 day period of both photometric and radial velocity variations of CH Cyg (Hinkle et al. 1993, 2009). The variations in the peak intensity of the SiO masers with a period of 2.5 yr implied their association with the pulsation motion of the M giant.

We also found a periodicity in the redshifted peak velocities of the SiO masers corresponding to the period of peak intensities (redshifted up to about $+40$ km s^{-1} with respect to the stellar velocity of the red giant -59.9 km s^{-1}). In the second cycle during 2015–2016, the SiO peak velocities became increasingly redshifted from about stellar velocity $V_{\rm LSR} = -60$ km s^{-1} (on 2012 December 27) to about $V_{\rm LSR} = -21$ km s^{-1} ($v = 2$, $J = 1 \rightarrow 0$ maser on 2018 March 8), according to observational dates.

There are two possible explanations for the 2.5 yr period of the SiO maser intensities and velocity behaviors. One is a periodic clumpy mass transfer in the inner binary system from the M giant to the low-mass companion due to a Roche lobe overflow at periastron. This kind of a periodic clumpy mass transfer may be stimulated by nonradial pulsation with a period of 750 days. Another possibility is a clumpy mass ejection from the M giant in a symbiotic binary system, and not a triple system, which is stimulated by nonradial pulsation with a period of 750 days.

This research was supported by the Basic Science Research Program through the National Research Foundation of Korea (NRF) funded by the Ministry of Education (2019R111A1A0105900) and by a Major Project Research Fund (2018–2020) of the Korea Astronomy and Space Science Institute (KASI). We are grateful to all of the staff members at KVN who helped to operate the array and the single-dish telescope and to correlate the data. The KVN is a facility operated by KASI, which is under the protection of the National Research Council of Science and Technology (NST). The KVN operations are supported by the Korea Research Environment Open NETwork (KREONET), which is managed and operated by the Korea Institute of Science and Technology Information (KISTI).

ORCID iDs

Se-Hyung Cho https://orcid.org/0000-0002-2012-5412
Haneul Yang https://orcid.org/0000-0001-6493-0619
Youngjoo Yun https://orcid.org/0000-0002-0822-2973

References

Belczyński, K., Mikolajewska, J., Munari, U., et al. 2000, A&AS, 146, 407
Bujarrabal, V., Mikoajewska, J., Alcolea, J., et al. 2010, A&A, 516, A19
Cho, S.-H., Yun, Y., Kim, J., et al. 2018, in Proc. IAU Symp. 336, Astrophysical Masers: Unlocking the Mysteries of the Universe, ed. A. Tarchi, M. J. Reid, & P. Castangia (Cambridge: Cambridge Univ. Press), 359
De Marco Orsola 2009, PASP, 121, 316
Deguchi, S., Koike, K., Kuno, N., et al. 2011, PASJ, 63, 309
Diamond, P. J., Kemball, A. J., Junor, W., et al. 1994, ApJL, 430, L61
Dilay, B., Howell, D. A., Cenko, S. B., et al. 2012, Sci, 337, 942
Doel, R. C., Gray, M. D., Humphreys, E. M. L., et al. 1995, A&A, 302, 797
Gaia Collaboration, Brown, A. G. A., Vallenari, A., et al. 2018, A&A, 616, A1
Goddi, C., Greenhill, L. J., Chandler, C. J., et al. 2009, ApJ, 698, 1165
Hachisu, Izumi, & Kato, Mariko 2001, ApJ, 558, 323
Han, S.-T., Lee, J.-W., Kang, J., et al. 2008, IJIMW, 29, 69
Han, S.-T., Lee, J.-W., Kang, J., et al. 2013, PASP, 125, 539
Hinkle, K. H., Fekel, F. C., Johnson, D. S., et al. 1993, AJ, 105, 1074
Hinkle, K. H., Fekel, F. C., Joyce, R. R., et al. 2009, ApJ, 692, 1360
Humphreys, E. M. L., Gray, M. D., Yates, J. A., et al. 2002, A&A, 386, 256
Iijima, T., Naito, H., & Narusawa, S. 2019, A&A, 622, A45
Issaoun, S., Goddi, C., Matthews, L. D., et al. 2017, A&A, 606, A126
Ivison, R. J., Seaquist, E. R., & Hall, P. J. 1994, MNRAS, 269, 218
Kamohara, R., Bujarrabal, V., Honma, M., et al. 2010, A&A, 510, A69
Karovska, M., Carilli, C., Mattei, J. A., et al. 2007, ApJ, 661, 1048
Markwardt, C. B. 2009, in ASP Conf. Ser. 411, Astronomical Data Analysis Software and Systems XVIII, ed. D. A. Bohlender, D. Durand, & P. Dowler (San Francisco, CA: ASP), 251
Mikoajewska, J., Balega, Yu., Hofmann, K.-H., et al. 2010, MNRAS, 403, L21
Mikolajewski, M., Mikoajewska, J., Khudyakova, T. N., et al. 1992, A&A, 254, 127
Owocki, S. P., Cranmer, S. R., & Blondin, J. M. 1994, ApJ, 424, 887
Pedretti, E., Monnier, J. D., Jacour, S., et al. 2009, MNRAS, 397, 325
Richter, L., Kemball, A., Jonas, J., et al. 2013, MNRAS, 436, 1708
Schmidt, M. R., Mikoajewska, J., & Hinkle, K. H. 2006, A&A, 446, 603
Seaquist, E. R., Ivison, R. J., & Hall, P. J. 1995, MNRAS, 276, 867
Skopal, A., Vanko, M., Pribulla1, T., et al. 2007, AN, 328, 909
Taylor, A. R., Seaquist, E. R., & Mattei, J. A. 1986, Natur, 319, 38
van Leeuwen, F. 2007, Hipparcos, The New Reduction of the Raw Data, Astrophysics and Space Science Library, Vol. 350 (Dordrecht: Springer)
Wong, K. T., Kaminski, T., Menten, K. M., et al. 2016, A&A, 590, A127
Yang, Haneul, Cho, Se-Hyung, Yun, Youngjoo, et al. 2020, MNRAS, 495, 1284
Yoon, Dong-Hwan, Cho, Se-Hyung, Kim, Jaeheon, et al. 2014, ApJS, 211, 15